Supporting information

Synthesis of nitrogen and sulfur doped carbon dots and application for fluorescence detection of Cd(II) in real water samples

Mingyu Tang,[a1] Xiaodong Liu,[a1] Nannan Zhang,[a] Jingyu Pang,[a] Yu Zou,[a] Fang Chai,[a,b]*

Hongbo Wu,[a] Lihua Chen*[b]*

[a] Key Laboratory of Photochemical Biomaterials and Energy Storage Materials, Heilongjiang Province; Key Laboratory for Photonic and Electronic Bandgap Materials, Ministry of Education, Harbin, 150025, Heilongjiang, China.

[b] Shandong Key Laboratory of Biochemical Analysis; College of Chemistry and Molecular Engineering, Qingdao University of Science and Technology, Qingdao 266042, PR China.

E-mails: fangchai@gmail.com, wuhongbo79@163.com, Lihuachen@qust.edu.cn

Celluar viability of the N&S CDs

The cytotoxicity of the N/S CDs was measured by the typical MTT assay.[1-3] In brief, HepG-2 cells (1×10^5 cells per well) suspension was supplemented with 5% CO_2 atmosphere at 37 °C and seeded into 96-well plates for 24 hours for attaining the spread morphology. After that, the other 24 hours incubation with the CDs in different concentrations was carried out in the culture medium. Then, 20 μL MTT (0.5 mg/mL) was added into each well after removing out the culture medium. Through 4 h further incubation, the culture medium was then removed ahead of additions of 100 μL DMSO. In the end, each sample's the optical density was measure down at 490 nm using a Microplate Reader. The viability (V_{HepG-2}) of the HepG-2 cells is calculated in terms of the following equation:

$$V_{HepG-2} = \frac{OD_{CDs}}{OD_{Con}}$$

where the OD_{Con} and OD_{CDs} are respectively referred to the absorbency of the cells incubated without and with the CDs. The evaluation was operated three times for precise result.

Before imaging measurement, HepG-2 cells were incubated through a routine cultivation process. Then, the different concentrations of N/S CDs solution was added into each well before a 4 h long cultivation. More, the cells were washed 3 times with PBS (1 mL per time) to remove the residual CDs and left 200 μL PBS for imaging. The cells were captured by a Fluorescence Inverted Microscope.

Determination of the fluorescence QY

The QY of the N&S CDs was determined by a widely recognized process.[4, 5] As a rule, quinine sulfate in 0.1 M H_2SO_4 aqueous solution was chosen to be the reference (QY: 54% at 340 nm). In order to abate the reabsorption effects, the solution of reference sample and N&S CDs were always diluted to keep the absorbance under below 0.1, respectively. The QY of the CDs is calculated following the equation below:

$$Q_{CDs} = Q_R\left(\frac{Grad_{CDs}}{Grad_R}\right)\left(\frac{\eta_{CDs}^2}{\eta_R^2}\right)$$

where subscripts R refers to quinine sulfate and N&S CDs, Q refers to the QY, Grad represents the gradient from the plot of integrated FL intensity / absorbance, and η is the refractive index of the solvent (water: 1.33).

Optimization of reaction parameters

As seen from Fig. S1 a and b and Fig. 3 c, in terms of reaction time, the CDs synthesized in 6 h provided the stronger fluorescence intensity. In the further exploration of the CDs in different contents of 2-MT in Fig. S1 c and d and Fig. 2 c, the results spectrum were vary widely no matter from the fluorescence intensity or excitation dependence, the amount of 0.50 mM 2-MT was optimized as the optimum reaction conditions for the CDs synthesis. And, the CDs prepared by 2-MT and TETA respectively were also explored. In Fig. S1 e and f, the fluorescence spectra were shown (e: 2-MT as raw material and g: T-acid as raw material), it is observed that the CDs synthesized by the mixture of the two shown better fluorescence performance than separately. It is co-doping procedure effectively improve the fluorescence property. In the further UV-vis absorbance, the content of 0.50 mM and reaction time of 6 h were further preferred with distinct peak shape (In Fig. S2 a and b). Then, as exhibited in Fig. S3, the TEM of the CDs prepared under different conditions were displayed. The TEM of CDs prepared by 2 h and 4 h were listed in Fig. S3 a and c, respectively, the morphology is not clear as a transition state (a, b: 2 h), and the CDs are insufficient hydrothermal carbonization (c, d: 4 h). In addition to this, In Fig. S3 e and g, the 2-MT in 0.25 mM and 1.00 mM were put into 10 mL TETA solution (V_{TETA}: V_{H_2O}=1:9). Fig. S3 e and f serves to shown the uneven distribution of the CDs. Fig. S3 g and h shown the in a state of heterogeneous aggregation and dispersion. The distribution of particle size of the CDs under different conditions was severally inserted at the bottom of each figure.

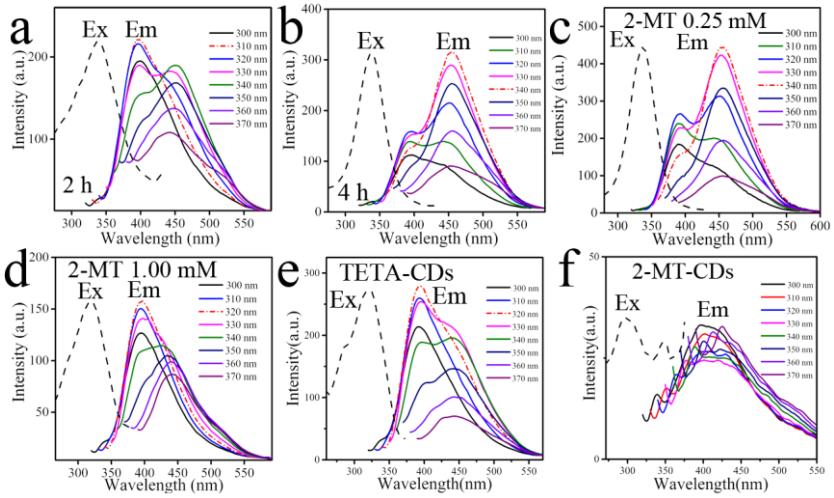

Fig. S1 Fluorescence spectra of the CDs synthesized under reaction time of 2 h (a), 4 h (b), 0.25 mM 2-MT (c), 1.00 mM 2-MT (d), raw material of TETA (e) and 2-MT (f).

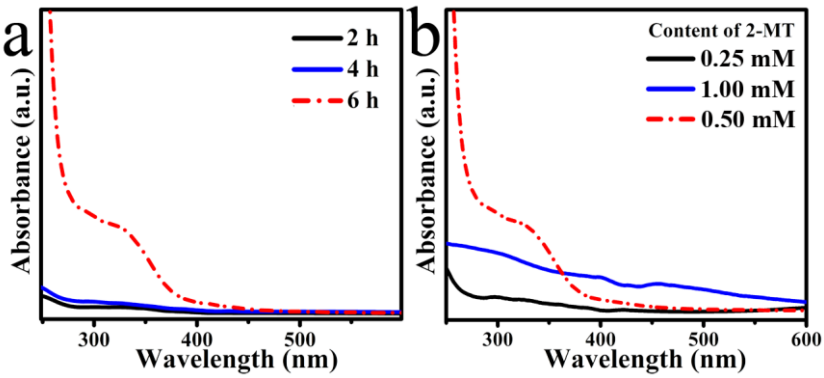

Fig. S2 UV-vis absorption spectrogram of the CDs synthesized under different conditions.

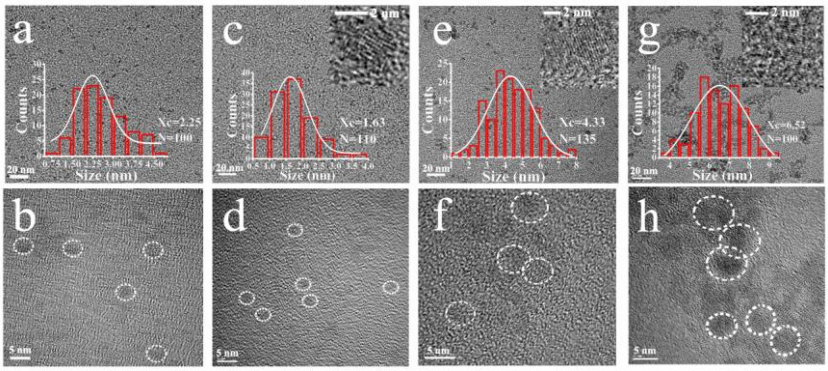

Fig. S3 Optimized TEM images of synthesized N/S co-doping CDs under the reaction time of 2 h (a) and 4 h (c), with the amount 2-MT of 0.25 mM (e) and 1.00 mM (g), inserts are the corresponding particle size distribution. (b), (d), (f), (h) are the corresponding TEM in the scale of 5 nm.

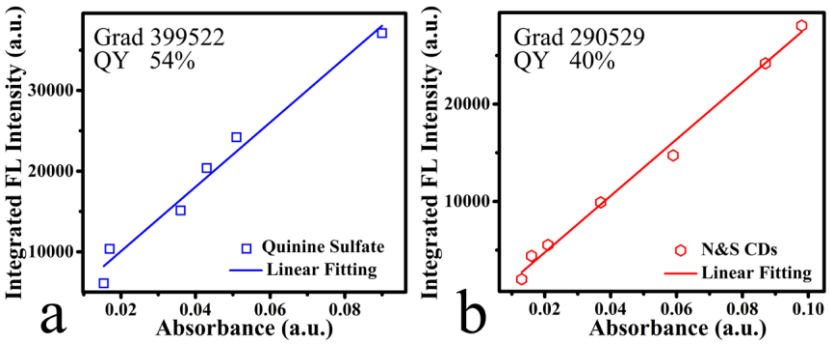

Fig. S4 Plots of integrated PL intensity of quinine sulfate (a) and N/S CDs as a function of optical absorbance at 340 nm (b)

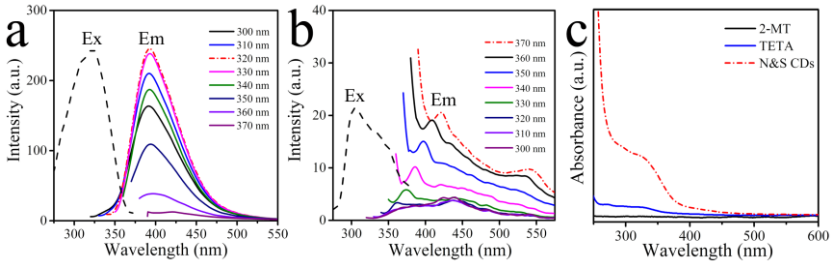

Fig. S5 Fluorescence spectra of TETA (a) and 2-MT (b) UV-vis absorption spectrogram of TETA, 2-MT and the CDs (c).

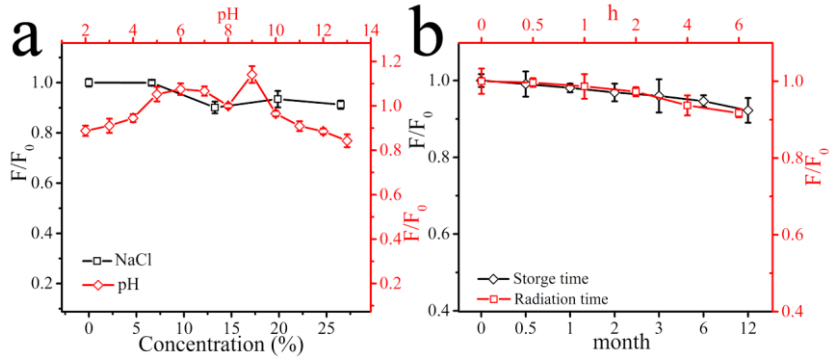

Fig. S6 Fluorescence spectrum stability under different salinity and pH (a), the fluorescence QE after unremitting UV radiation exposure and 12 months storage (b).

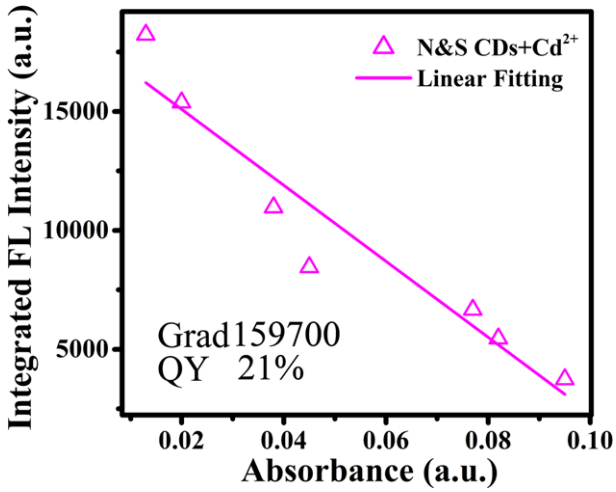

Fig. S7 The quantum yield of the N&S CDs after adding selective metal ion Cd^{2+}

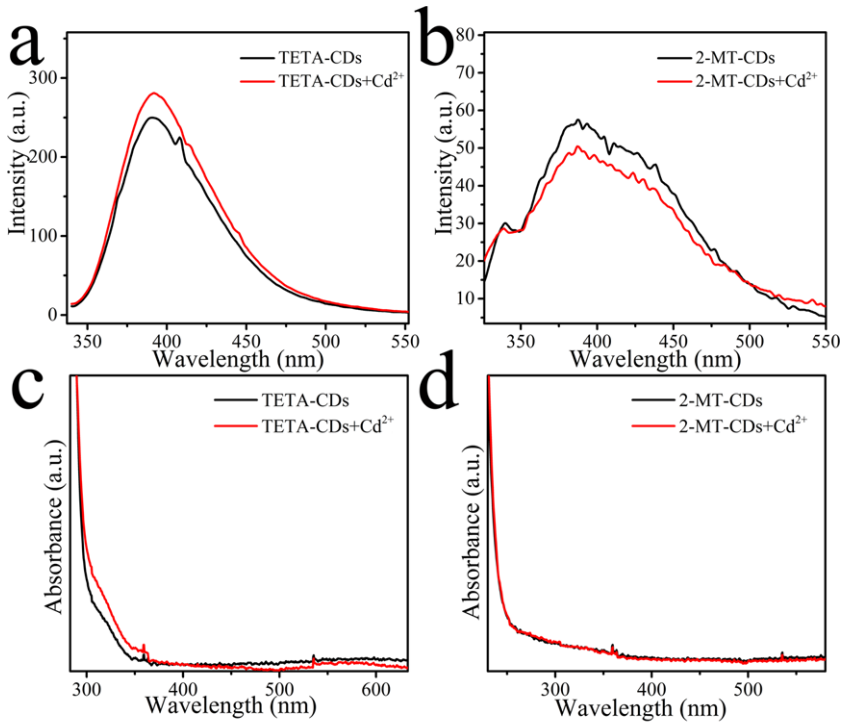

Fig. S8 The FL spectra (a, b) and UV-Vis (c, d) spectra of the TETA-CDs and 2-MT CDs upon the addition of Cd^{2+} ion.

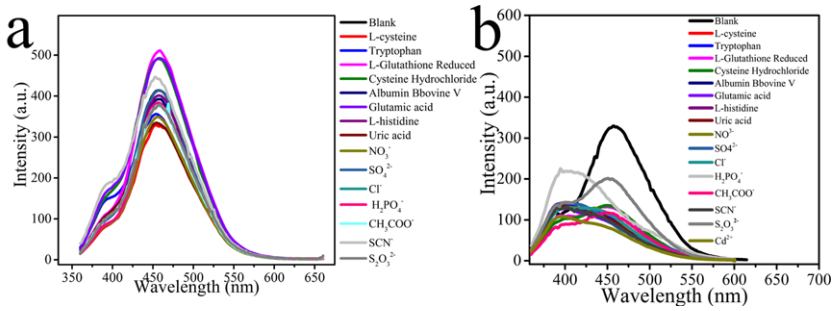

Fig. S9 The FL spectra of the N&S CDs upon the addition of anions and biomolecules (a) after introducing the 100 μM of Cd^{2+} in the samples (b).

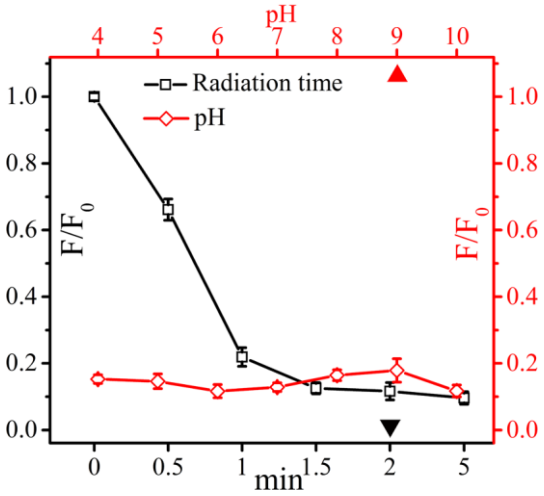

Fig. S10 QE of the CDs based probe towards Cd^{2+} under different pH and radiation time

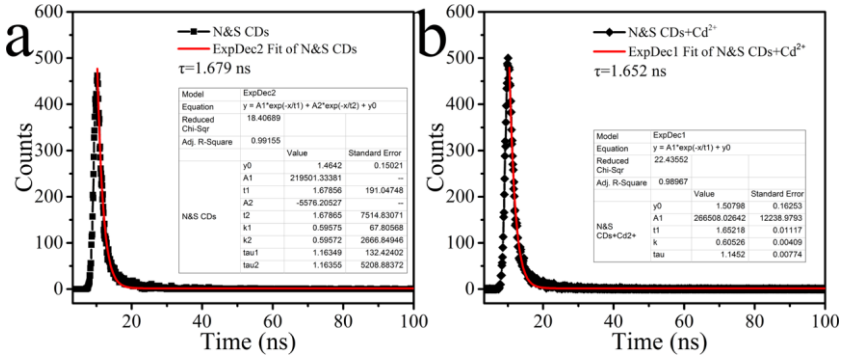

Fig. S11 Fluorescence decay traces of N&S CDs (a) and N&S CDs+Cd^{2+} system (b).

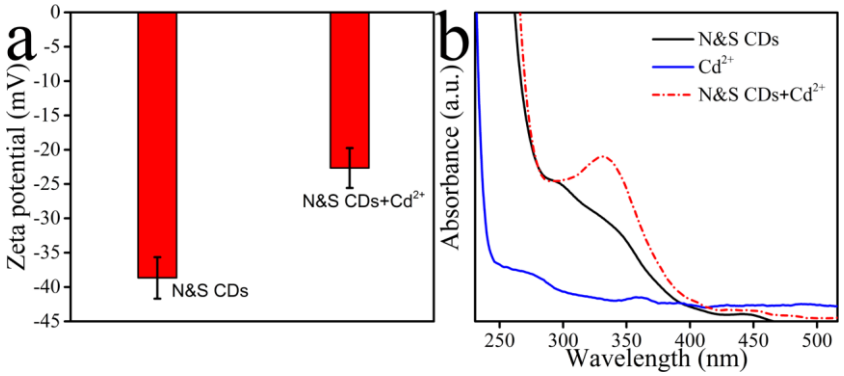

Fig. S12 The zeta potential values of N&S CDs and N&S CDs+Cd^{2+} (a) and UV-vis absorption spectrum of N&S CDs with and without Cd^{2+} (b).

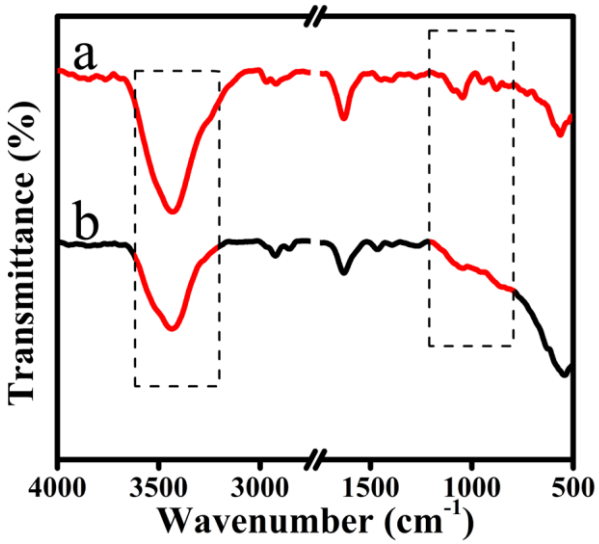

Fig. S13 FT-IR spectra of N/S CDs with the absence (a) and presence of Cd^{2+} (b).

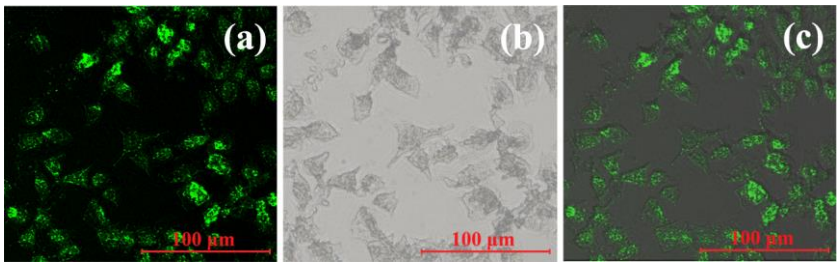

Fig. S14 bright field confocal images of CDs in HepG-2 cells (a); black field confocal images of the CDs in HepG-2 cells (b); the merge of (a) and (b), (c).

Table S1. FWHM of the synthesized CDs

CDs Sample	N/S CDs 2-MT-0.25 mM	N/S CDs 2-MT-1.00 mM	N/S CDs 2 h	N/S CDs 4 h	TETA-CDs	2-MT-CDs
FWHM	92	81	90	98	99	16

Table S2. The fluorescence effect compared to Cd^{2+} of the different ions in the selectivity assay.

Ion	Blank	Ag^{+}	Ba^{2+}	Ca^{2+}	Co^{3+}	Cr^{3+}	Cr^{6+}	Cu^{2+}	Fe^{2+}
Relative quenching rate %	0	29.9	27.8	37.8	6.69	38.0	27.1	23.0	36.4
Ion	Fe^{3+}	Hg^{2+}	Mg^{2+}	Mn^{2+}	Ni^{2+}	Pb^{2+}	Zn^{2+}	Cd^{2+}	
Relative quenching rate %	35.3	5.02	37.6	8.90	40.13	42.7	8.85	1	

Table S3. The relative error of ions in the interference assay.

Interference ion	Blank	Ag^{+}	Ba^{2+}	Ca^{2+}	Co^{3+}	Cr^{3+}	Cr^{6+}	Cu^{2+}	Fe^{2+}
Relative Error (%)	1.24	3.53	4.11	3.62	3.72	5.71	4.71	4.55	8.71
Interference ion	Fe^{3+}	Hg^{2+}	Mg^{2+}	Mn^{2+}	Ni^{2+}	Pb^{2+}	Zn^{2+}	Cd^{2+}	
Relative Error (%)	2.44	5.58	6.61	2.65	1.17	3.14	2.33	1.18	

Table S4. Comparison of several types of probe for the Cd^{2+} detection.

Methods	Probe type	LOD (nM)	Ref.
Peptide	**Fluorescence**	**27.5**	**6**
Phenanthroline derivatives	**Spectroscopy**	**15.0**	**7**
BiSn nanoparticles	**Electrochemical determination**	**3.0**	**8**
Caboxylic acid hydrazide	**Colorimetry**	**100.0**	**9**
Au NPs	**Colorimetry**	**20.0**	**10**
Hydroxylquinoline-benzothiazole conjugate	**Fluorescence**	**100.0**	**11**
Dopamine-inspired Au	**SERS**	**10.0**	**12**
N&S CDs	**Fluorescence**	**18.0**	**This work**

Table S5. The quantitation report of the ICP in the waste water.

Element	Sample	ISTD	CPS or Ratio	Concentration	RSD (%)	Time (sec)
Cd^{2+}	Tap water	115	8.09E-5 P	4.98E-01 ppb	7.30	6.00
Cd^{2+}	Waste water.	115	8.37E-6 P	<0.00 ppb	3.06	6.00
Cd^{2+}	Yalv River	115	5.77E-6 P	<0.00 ppb	1.33	6.00
Cd^{2+}	Yellow Sea	115	2.89E-6 P	4.86E-02 ppb	0.42	6.00

Reference

1. S. Konar, B. N. P. Kumar, M. K. Mahto, D. Samanta, M. A. S. Shaik, M. Shaw, M. Mandal and A. Pathak, *Sensors and Actuators B: Chemical*, 2019, **286**, 77-85.
2. L. Li, L. Shi, Y. Zhang, G. Zhang, C. Zhang, C. Dong, H.-Z. Yu and S. Shuang, *Talanta*, 2019, **196**, 109-116.
3. Y. Hu, Z. Chen, F. Lai and J. Li, *Journal of Materials Science*, 2019, **54**, 8627-8639.
4. Q. Hu, L. Gao, S. Q. Rao, Z. Q. Yang, T. Li and X. Gong, *Food chemistry*, 2019, **280**, 195-202.
5. N. Jing, M. Tian, Y. Wang and Y. Zhang, *Journal of Luminescence*, 2019, **206**, 169-175.
6. P. Wang, K. Chen and Y. Ge, *Journal of Luminescence*, 2019, **208**, 495-501.
7. R. Satheeshkumar, R. Rajamanikandan, M. Ilanchelian, K. Sayin and K. J. R. Prasad, *Spectrochimica acta. Part A, Molecular and biomolecular spectroscopy*, 2019, **221**, 117196.
8. Y. Chen, D. Zhang, D. Wang, L. Lu, X. Wang and G. Guo, *Talanta*, 2019, **202**, 27-33.
9. V. Tekuri and D. R. Trivedi, *Analytica chimica acta*, 2017, **972**, 81-93.
10. J. Qiu, Z. Li, L. Miao, H. Wang, Y. Zhang, S. Wu, Y. Zhang, X. Li and A. Wu, *The Analyst*, 2019, DOI: 10.1039/c9an00836e.

11. Z. N. Lu, L. Wang, X. Zhang and Z. J. Zhu, *Spectrochimica acta. Part A, Molecular and biomolecular spectroscopy*, 2019, **213**, 57-63.
12. J. Du and C. Jing, *Analytica chimica acta*, 2019, **1062**, 131-139.